



# A Novel Microfluidic Pressure Sensor for Traditional Chinese Medicine (TCM) Pulse Data Collection and Analysis

Zhu Hong<sup>1</sup><sup>a</sup>, Lin Liutong<sup>1</sup><sup>b</sup>, Er Jui Pin<sup>1</sup><sup>c</sup>, James Wong<sup>2</sup> and Sun Lingling<sup>1</sup><sup>d</sup>

<sup>1</sup>Healthcare Engineering Centre, School of Engineering, Temasek Polytechnic, 21 Tampines Ave. 1, Singapore

<sup>2</sup>TP-HRG Robotics Innovation Centre, School of Engineering, Temasek Polytechnic, 21 Tampines Ave. 1, Singapore

**Keywords:** Wearable Electronics, Microfluidic Pressure Sensor, Traditional Chinese Medicine, TCM Pulse Analyzer.

**Abstract:** Recently, we developed a novel microfluidic pressure sensor which can accurately sense and collect human wrist arterial pulse signals to be used in a wearable TCM pulse analyzer enabled with artificial intelligence for self-monitoring of cardiovascular disease. Various micro tactile sensor structures had been explored and fabricated using in-house microfabrication facilities. The connection between the parameters of sensor and its output has been investigated and found that the parameters of pressure sensor had great influence on its performance. An easy-to-use mechanical structure to hold the sensor and pulse signal reading and processing electronics on both hardware and firmware have also been designed and fabricated.

## 1 INTRODUCTION

### 1.1 Significance of TCM Pulse Diagnosis

TCM has been practiced for more than 2,500 years. The 11th revision of the World Health Organization's (WHO) International Statistical Classification of Diseases and Related Health Problems (ICD-11), which was released on 18 Jun 2018, included TCM for the first time. A disease classification system, based on TCM was established in the ICD-11. It is of great practical and historical significance to promote the integration of TCM and the medical and health systems in the world, and to lay the foundation for the world to understand and use TCM.

TCM pulse diagnosis has been used by TCM physicians to assess patients' health conditions. As shown in Figure 1, a TCM physician palpates six locations, three on each wrist, with the three points called "Cun" (寸), "Guan" (关) and "Chi" (尺) at three pulse depths called "Fu" (浮), "Zhong" (中) and "Chen" (沉) and describes pulses in terms of various characteristics. By comparing the pulses, the health

status of individual organs and the whole body can be determined (Meng et al., 2001 and Wang, 2000).

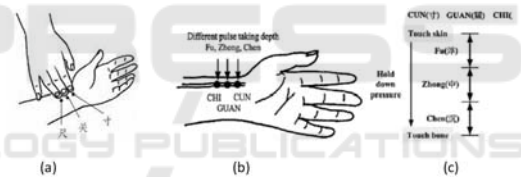






Figure 1: An illustration of the TCM palpation: (a) A TCM physician using his 3 fingers (index, middle, ring finger) to collect pulse signal, (b) 3 pulse-taking positions (Cun, Guan, and Chi) and (c) 3 pulse-taking depths (Fu, Zhong and Chen).

The basic rationale behind TCM pulse diagnosis is that pathologic changes in the body are reflected in the radial pulse. This premise is supported by western clinical research studies, which have found evidence for loss of arterial elasticity and alterations in pulse amplitude, rhythm, and shape in patients with cardiovascular disease, hypertension, diabetes, etc. (Malinauskas et al., 2013). In several articles, the pulse wave is described as the superposition of a forward traveling wave caused by the ventricular output of blood and a phase-shifted backward traveling wave reflected from the peripheral blood

<sup>a</sup>  <https://orcid.org/0000-0003-2574-6258>

<sup>b</sup>  <https://orcid.org/0000-0003-2401-3853>

<sup>c</sup>  <https://orcid.org/0000-0002-7071-9462>

<sup>d</sup>  <https://orcid.org/0000-0002-9465-7198>

vessels (Malinauskas et al., 2013; Jeon et al., 2011 and Shu, 2007). It was indicated that the forward traveling component is correlated with information about the heart itself and the backward traveling wave contains information about the arterial tree and the organs it flows through (Malinauskas, et al., 2012). Therefore, the pulse diagnosis has important clinical values on diagnosing diseases of various organs and assessing the patient's status holistically.

## 1.2 Modern Scientific Approaches on the Objectification of TCM Pulse Diagnosis

Despite its importance, TCM pulse diagnosis is subjective and mysterious as it is based purely on the physicians' finger feels. The wrist pulse characteristics are mainly described qualitatively and cannot be clearly defined quantitatively. The fuzziness and ambiguity of pulse concepts make it difficult to study and master pulse diagnosis. As long as pulse diagnosis remains in the realm of fingertip-reading, it will be a difficult skill to master and have a great deal of subjectivity in interpretation.

Objectification of the pulse diagnosis is highly desired. Over the last two decades, considerable research efforts have been put into the attempt to objectify the pulse diagnosis. Various pulse diagnosis instruments have been developed to obtain pulse signals quantitatively (Zhang et al., 2011; Luo et al., 2012 and Hu et al., 2012), and many analytical methods have been proposed for exploring the mechanism of pulse conditions and correlations with diseases (Jeon et al., 2011; Wei et al., 2009, Wang et al., 1997; Liao et al., 2012). These modern practices of pulse diagnosis have revived the TCM and demonstrated the value of pulse diagnosis is not only non-invasive diagnosis but also an early prediction of diseases. Yi-Chia Huang (Huang et al., 2019) has identified predictive factors of pulse spectrum to increase the prediction rate of coronary artery disease (CAD) diagnosis in patients with chest pain or angina pectoris prior to cardiac catheterization. For predicting the attack of type 2 diabetes, an algorithm developed by Yiming Hao (Hao et al., 2019) achieved an accuracy of 96.35%. Many other studies also provide important evidence of using pulse characteristics for various disease diagnoses, such as lung cancer recognition (Zhang et al., 2018), atopic eczema diagnosis (Liou et al., 2011), fatty liver disease diagnosis (Wang et al., 2015), dyspepsia and the rhinitis detection (Huang et al., 2011).

## 1.3 The Interest in Developing Wearable TCM Pulse Analyzer

The pulse analysers currently developed are mainly desktop instruments (Luo et al., 2012). However, the desktop pulse analysers are cumbersome and need complicated pressure adjustment for pulse taking, which prevents them from being extensively used by clinicians and patients, especially for continuously monitoring the pulse signals. Continuous monitoring of the pulse signal is preferable for many disease diagnoses and early prediction of risks. With continuous monitoring, the history of a health condition related to the diseases can be retrieved for helping the diagnosis process, and certain important physiological and pathological characteristics will not be missed.

In the prospect of the increase in demand, developing a low-cost, wearable pulse analyzer that can offer continuous monitoring, immunizes mechanical and electronic noises, as well as displays some basic diagnostic results is becoming one of the most popular research topics (Wang et al., 2016 and Goyal et al., 2017). However, the wearable pulse analysers currently available in the market or under development can only exert non-adjustable pressure, which is inconsistent with the palpation theory in TCM. There is no easy-to-use, wearable TCM pulse analyzer which can palpate at three positions and three depths.

## 1.4 Proposed Wearable TCM Pulse Analyzer

We aim to develop a TCM pulse collector or analyser to collect the pulse signal at three positions (Cun, Guan, Chi). A simple mechanical structure will hold the pulse sensor and to control the exerting pressure at three levels (Fu, Zhong, Chen) according to TCM theory has been designed and fabricated. Both electronics and firmware of the pulse analyser have been developed for pulse signal reading and processing. Various filters and algorithms have been explored to de-noise and remove signal drift. The signal processing sub-system further controls the adjustment of the pulse signal collection at three positions (Cun, Guan, Chi) and three depths (Fu, Zhong, Chen).

## 2 DESIGN AND FABRICATION

### 2.1 Sensor Fabrication

The flexible microfluidic pressure sensors have been designed with different patterns and or geometry parameters (microfluidic channel width ranging from 200  $\mu\text{m}$  to 500  $\mu\text{m}$ , channel spacing ranging from 200  $\mu\text{m}$  to 500  $\mu\text{m}$ ). Plastic masks with different patterns have been printed to fabricate microfluidic sensor SU8 mould using lithography technique. Figure 2 shows some typical designs of the sensor. Figure 3 shows a SU8 mould for flexible sensor fabrication using lithography process.

We developed both the bonding process of Ecoflex and Polydimethylsiloxane (PDMS) to Polyethylene terephthalate (PET) film with metal electrodes. The sensors made by bonding PDMS to PET film have poor sensitivity compared with sensors made by bonding Ecoflex to PET film, due to the higher Young's modulus of PDMS than Ecoflex.

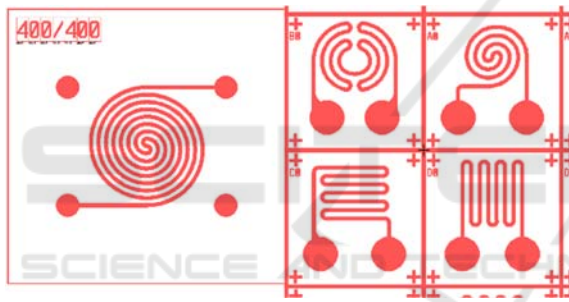


Figure 2: Some designs of the flexible microfluidic pressure sensors.

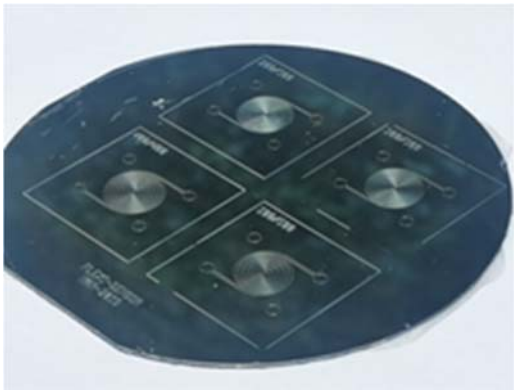


Figure 3: A 4-inch size SU8 mould for flexible sensor fabrication.

The flexible microfluidic sensor fabrication process is composed of following several individual steps as shown below:

a) SU8 mould fabrication process, including spin coating of SU8, prebaking of the SU8, ultraviolet (UV) exposure lithography pattern formation, post-exposure baking of the SU8 and SU8 pattern development process.

b) Ecoflex sensor moulding by mixing the Ecoflex A and B solution, pouring the Ecoflex solution on the SU8 mould, degassing the Ecoflex liquid in the vacuum oven, baking at 70  $^{\circ}\text{C}$  for 1hour.

c) Demoulding of the Ecoflex from the SU8 mould and separation of the individual Ecoflex sensor from the whole piece of Ecoflex.

d) Reactive Ion Etching (RIE)  $\text{O}_2$  plasma treatment on both surfaces of Ecoflex and PET film, or by hand-held Corona Treaters having air plasma treatment on both surfaces of Ecoflex and PET film. The RIE is a standard microfabrication machine,  $\text{O}_2$  plasma treatment by RIE is a more standard method.

e) Bonding of the Ecoflex sensor to the PET film with metal electrode immediately after the surface treatment, which is the most critical step and with the lowest yield in all steps of the fabrication steps.

f) Baking of the bonded sensor at 80  $^{\circ}\text{C}$  for 30 mins to further strengthen the bonding strength between Ecoflex and PET film.

g) Injection of the Eutectic GaIn liquid metal into the channel between the Ecoflex and PET film and sealing of the injection hole by Ecoflex liquid; h) Soldering of the electrically conductive cloth to the PET film.

### 2.2 Testing Methods of the Pressure Sensor

Characterization of the sensor was carried out by measuring the pressure sensor's electrical resistance output versus the force applied to the sensor. All the fabricated microfluidic pressure sensors are tested using mainly two equipment, force load machine (A) and a digital multimeter (B) as shown in Figure 4. The force load machine allows a varied force from 0 N to 5 N which corresponds to the force generated by the

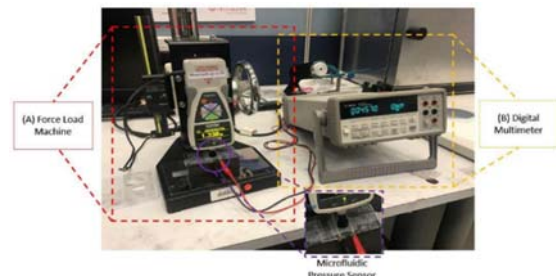


Figure 4: Testing setup for microfluidic pressure sensor.

human pulse on the wrist to be applied onto the pressure sensor. The multimeter allows the measurement of the resistance between the electrode when a force is applied.

### 3 RESULTS AND DISCUSSION

#### 3.1 Sensor Parameters and Its Output

Figure 5 shows the structure of the microfluidic pressure sensor. The working principle of the microfluidic pressure sensor is based on the resistive mechanisms where an external force applied to the device causes a resistivity change in the conducting path of the microfluid. The conductivity of the microfluid liquid is determined by the eutectic metal in the channel. When under pressure, the channel height will become smaller, the channel length will become longer, thus the resistance of the liquid metal inside the channel will become larger under pressure. An external force deforms this conductive path which results in an increase in resistance of the sensor.

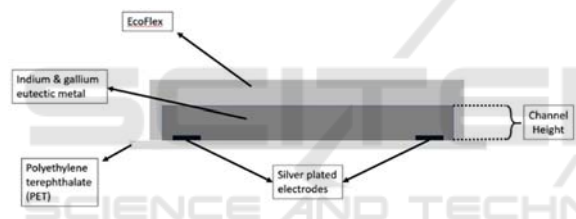


Figure 5: The structure of the microfluidic pressure sensor.

Figure 6 shows the cross-section diagram of the microfluidic pressure sensor. The fabrication parameters of the sensor include channel width, channel spacing, channel height, and Ecoflex thickness or height. Below, the impacts of the different parameters of the sensors on the electrical resistance between the electrode are discussed.

It is found that the sensors with small dimensions like 8 mm x 8 mm were very difficult to fabricate, due to the poor bonding strength between the Ecoflex and PET film. Sensors with bigger sizes have better yields in fabrication. It is not recommended to fabricate very small sensors like 8 mm X 8 mm in size. Currently, our sensor with good yields is the one with a circular channel shape with dimension 15 mm X 22 mm.

Figure 7 shows a fabricated microfluidic pressure sensor, composed of a microchannel filled with liquid metal between the Ecoflex and PET film.

Figure 8 shows the effects of the Ecoflex thickness on the output resistance with same channel width and spacing 500 μm/500 μm. channel height

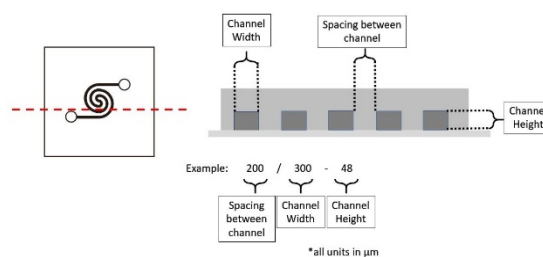


Figure 6: Cross-Sectional diagram of microfluidic pressure sensor.

about 60 μm. It can be seen clearly, while the thickness of the Ecoflex decreased from 1.411 mm to 0.858 mm from top curve to the bottom curve, the gradient of the force- resistance curve decreased dramatically, which means the sensitivity of the sensor decreased while thickness of the sensor increased. This is reasonable, as a thin Ecoflex tends to have more deformation when under same pressure, which results in a higher change of the resistance of the metal liquid, thus a better response. When the thickness of the sensor was about 1.4 mm, the sensor’s resistance almost has no change under pressure.



Figure 7: Fabricated microfluidic pressure sensor.

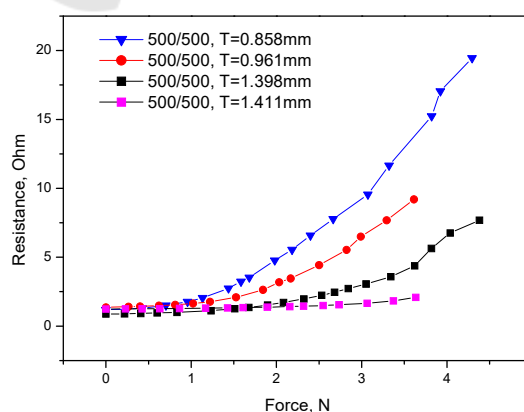


Figure 8: Electrical resistance of pressure sensor with same channel width and spacing 500 μm /500 μm and same channel height 60 μm but with different sensor thickness.

Figure 9 shows the electrical resistance response of the pressure sensor with different channel widths and spacings but with the same channel height and around same sensor thickness. It can be seen clearly that sensor with channel dimension of 200 $\mu\text{m}$  width and 300  $\mu\text{m}$  spacing has the highest gradient of the input and output curve, and it is the most sensitive one.

Even though the sensor with small channel width and space has better resistance response. We still did not fabricate any sensor with channel width or space less than 200  $\mu\text{m}$ . The main reason is the low yield when fabricating sensors with channel dimension less than 200  $\mu\text{m}$ . The smallest sensor dimension we made in this experiment is 200  $\mu\text{m}$  channel width and 300 $\mu\text{m}$  spacing. Since we are looking for a sensor with better sensitivity, we decided to focus on the fabrication of sensor with channel width and spacing of 200 and 300  $\mu\text{m}$  respectively.

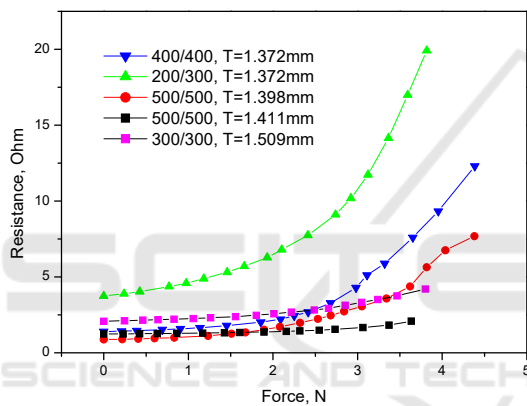


Figure 9: Electrical resistance of pressure sensor with different channel width and spacing ranging from 500/500  $\mu\text{m}$  to 200/300  $\mu\text{m}$  but with same channel height 60  $\mu\text{m}$  and about same sensor thickness.

We have also carried out the fabrication process for sensor with different channel height but with same channel pattern (same channel width and spacing) and same sensor thickness. The experiment results shows that sensor with low channel height has better response under pressure, which is also reasonable.

Currently, the yield of the fabrication process is good, but still the process is challenging. The most challenging step in the fabrication process is the bonding of Ecoflex to the PET film. As we know, in microfabrication the bonding process is the most challenging step in all processes since it is greatly related to the surface condition or surface state of the two bonding parts. The surface condition is difficult to control, and hence the bonding process is difficult to control. The bonding strength of PDMS to PET film is better than that of Ecoflex to PET film. During

the experiments, two things need to be prioritized. The first one is to optimize the bonding process, how to make it stable, and with high yield, while the second one is to design for manufacturability, i.e., how to design the sensor structure or pattern for a better yield and a sensor with high stability in usage.

Among the different designs of the sensor, based on the testing results, it is concluded that to fabricate a microfluidic sensor with high sensitivity, the channel width, the channel spacing, the channel height, the sensor height, should be small, which is limited by the current microfabrication process. In our case, the microfluidic pressure sensor with physical design of channel width 200  $\mu\text{m}$ , channel spacing 300  $\mu\text{m}$ , channel height about 60  $\mu\text{m}$ , and sensor height 1mm has the best sensitivity.

### 3.2 Physical Design and Mechanical Structure of the Wearable TCM Pulse Reader

In this wearable TCM pulse reader, a microfluidic force sensor is fixed in a housing. When put on and properly located on the wrist, the pulsation of radial artery will be transferred through a mechanism to the sensor, causing the variation of resistance of the sensor. The variation of the resistance would be converted into varying voltage signals, which would be picked up by a control board connected to it. Signal would be processed and analysed by an intelligent system to diagnose or predict certain diseases from it. Hence, proper mechanism, structure, and housing is one of the crucial parts of the pulse reader.

Two signal wires connect the sensor to the control board, with one end connected to the sensor, and the other end to a snap button. This snap button in turn connects to another half of the snap button, which is connected to the control board with another piece of wire. The signal wires are wrapped in plastic film for protective and easy handling purposes.

### 3.3 Pulse Signal Collection, Processing Electronics and Firmware

A block diagram for the pulse data acquisition, signal processing, and machine learning is shown in Figure 10. The microcontroller system includes an anti-aliasing filter before data sampling and some instrumentation front-end electronics before the analog-to-digital conversion (ADC). Our sensors have very low impedance, from a fraction of an ohm in the unobstructed state to a few tens of ohms under pressure. The pulses on the wrist only change the resistance by a few milliohms. A constant excitation

current to the sensor, a precision reference resistor, differential inputs to ADC with differential and common-mode filtering may be necessary. User’s breathing motion and the air pressure changes will cause some signal drift (baseline wander). The removal of such drift, together with other noise if existing, will be done in the firmware, possibly using some wavelet decomposition algorithms. The clean pulse signals will then be used in the following processes:

- a) The measured air pressure value will be used to control the air-pump and air-release valve to adjust the pressure on each sensor for pulse taking.
- b) Pulse waveform can be displayed on the device monitor. Additionally, the signals can be transmitted via Bluetooth Low Energy (BLE) to a mobile phone and shown on it. The mobile phone can further connect to the Cloud through Wi-Fi or GSM for further signal analysis.
- c) The 17 pulse features (or potentially just the key required features for heart disease diagnosis in the initial prototypes) will be extracted, and features pertaining to heart diseases will be selected for diagnosis classification using artificial intelligence technology.

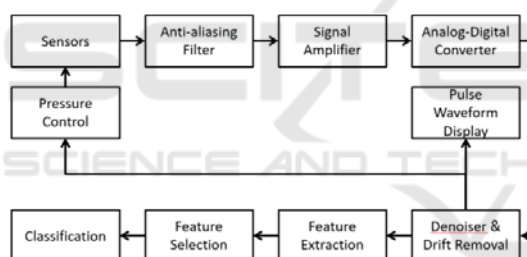


Figure 10: A block diagram of the pulse signal acquisition, signal processing, and classification.

### 3.4 Preliminary Results on Pulse Signal Acquisition

A preliminary prototype built using an ESP32-PICO-D4 microcontroller with a 24-bit ADS1220 ADC chip connected to our in-house fabricated microfluidic sensor has shown some promising results. Figure 11 shows the pulse signals collected from one subject in one measurement session, clearly showing different pulse patterns at different depths/pressures. The air pressure was not controlled and maintained in this test, and the signal drift was removed with an algorithm in the firmware. The signals were not too noisy at 20 Hz sampling rate. The sensor resistance varies by 0.3 to 1 milliohm with the arterial pulse.

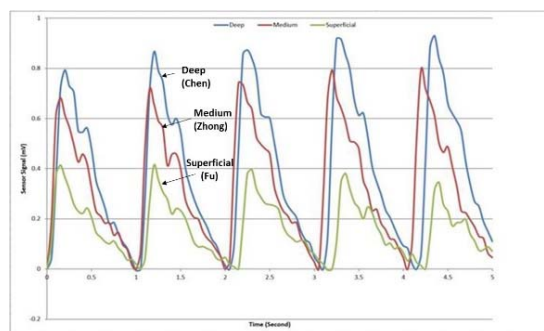


Figure 11: Pulse signal acquisition and data processing electronics device and human pulse signal collection.

## 4 CONCLUSIONS

A novel microfluidic pressure sensor with good performance which can sense the human pulse signal has been developed using microfabrication process. The effects of different sensor design patterns and different sensor parameters such as Ecoflex thickness, channel height, channel width and spacing on its output performance have also been investigated. The following parameters: Ecoflex thickness less than 1mm, 200 μm channel width, 300 μm channel spacing and 60 μm channel height is an optimized sensor parameter which can produce sensor with a good sensitivity and high yield in fabrication.

A wearable TCM pulse analyzer based on the microfluidic pressure sensor, which can accurately sense and collect wrist arterial pulse signals has also been fabricated. The mechanical structure of the pulse analyser, the signal processing electronics both on hardware and software have also been developed, which can be applied in future diagnosis of diseases according to TCM theory.

In future work, we will also develop pulse pattern feature extraction, selection, and classification models with a premier focus on cardiovascular disease diagnosis based on TCM theory. We will use techniques such as time-domain feature extraction, wavelet decomposition, and ensemble-learning method combining deep Convolutional Neural Network (CNN) and Fuzzy Neural Network (FNN) to enhance the predictive performance.

## ACKNOWLEDGEMENTS

We thank Singapore Ministry of Education (MOE) Translation and Innovation Fund (TIF) to support this project. We also acknowledge Prof Lim Chwee Teck,

Dr. Yeo Joo Chuan and their research team from National University of Singapore (NUS) for all helpful discussions and valuable suggestions.

## REFERENCES

- Meng, J., Zhou, Z. (2001). *Introduction to Chinese medicine*, Jyin Publishing Company, Taipei.
- Wang, L. (2000). *Diagnostics of traditional Chinese medicine*, Publishing House of Shanghai University of Traditional Chinese Medicine, Shanghai.
- Malinauskas, K., Palevicius, P., Ragulskis, M., Ostasevicius, V., Dauksevicius, R. (2013). Validation of non-invasive MOEMS-assisted measurement system based on CCD sensor for *radial pulse analysis*. *Sensors* 13 (4); 5368–5380.
- Jeon, Y., Kim, J., Lee, H. et al. (2011). A clinical study of the pulse wave characteristics at the three pulse diagnosis positions of Chon, Gwan and Cheok. *Evidence-Based Complementary and Alternative Medicine*, vol. 2011, Article ID 904056.
- Shu, J. (2007). Developing classification indices for Chinese pulse diagnosis, *Complement. Ther. Med.* 15 (3) 190–198.
- Malinauskas, K., Ostasevičius, V., Daukševičius, R., Jūrenas V. (2012). Non-invasive micro-opto-electro-mechanical system adaptation to radial blood flow pulse and velocity analysis. *Mechanics* 18 (4) 479–483.
- Zhang, J., Wang, R., Lu, S., Gong, J., Zhao, Z., Chen, H., Cui, L., Wang, N., Yu, Y. (2011). EasiCPRS: Design and implementation of a portable Chinese pulse-wave retrieval system. *Proceedings of the 9th ACM Conference on Embedded Networked Sensor Systems*, 149–161.
- Luo, C., Chung, Y., Hu, C., et al. (2012). Possibility of quantifying TCM finger-reading sensations: I. Bi-sensing pulse diagnosis instrument. *Eur J Integr Med*; 4: e255–62.
- Hu, C., Chung, Y., Yeh, C., Luo, C. (2012) Temporal and spatial properties of arterial pulsation measurement using pressure sensor array. *Evidence Based Complement Alternat Med*; Vol. 2012, Article ID 745127.
- Wei, C., Huang, C., Liao, T. (2009). The exponential decay characteristic of the spectral distribution of blood pressure wave in radial artery. *Computers in Biology and Medicine*, 39:453–459.
- Wang, Y., Chang, C., Chen, J., Hsiu, H., Wang, W. (1997). Pressure wave propagation in arteries. *IEEE Eng Med Biol Mag*, 16:51–56.
- Y. Liao, H. Chen, C. Huang, M. Ho et al. (2012). The pulse spectrum analysis at three stages of pregnancy. *J Alternat Complement Med*, 18:382–386.
- Huang, Y., Chang, Y., Cheng, S., et al. (2019). Applying pulse spectrum analysis to facilitate the diagnosis of coronary artery disease, *Evidence-Based Complementary and Alternative Medicine*, vol. 2019, Article ID 2709486.
- Hao, Y., Cheng, F., Pham, M., et al. (2019). A non-invasive, Economical, and instant-result method to diagnose and monitor type 2 diabetes using pulse wave: case-control study. *JMIR Mhealth Uhealth*, vol. 7, iss. 4, e 11959.
- Zhang, Z., Zhang, Y., Yao, L., et al. (2018). A sensor-based wrist pulse signal processing and lung cancer recognition. *J. Biomed Inform*, 79, 107-116.
- Liou, J., Huang, C., Chiu, C., et al. (2011). Differences in pulse spectrum analysis between atopic dermatitis and nonatopic health children, *The Journal of Alternative and Complementary Medicine*, vol 17, no. 4, pp. 325-328.
- Wang, N., Yu, Y., Huang, D. (2015). Pulse diagnosis signals analysis of fatty liver disease and cirrhosis patients by using machine learning. *The Scientific World Journal*, Volume 2015, Article ID 859192.
- Huang, C., Chang, H., Kao, S., et al. (2011). Application of sphygmography to detection of dyspepsia and the rhinitis. *The American Journal of Chinese Medicine*, vol. 39, no. 2, pp. 271–285.
- Wang, D., Krusienski, D., Hao, Z. (2016). A Flexible PET-based wearable sensor for arterial pulse waveform measurement. *Proceedings of the 9th International Joint Conference on Biomedical Engineering Systems and Technologies (BIOSTEC 2016), Volume 1: BIODEVICES*, pages 66-75.
- Goyal, K., Agarwal, R. (2017). Pulse based sensor design for wrist pulse signal analysis and health diagnosis. *Biomedical Research*; 28 (12): 5187-5195.